

Reachability Analysis
**AN OFF-LINE METHOD FOR BASE PLACEMENT
IN MOBILE MANIPULATORS**

Homayoun Seraji
Jet Propulsion Laboratory
California Institute of Technology
Pasadena, CA 91109

Abstract

This paper addresses the problem of base placement for mobile robots, and proposes a simple off-line solution to determine the appropriate base locations from which the robot can reach a target point. For robots with one degree-of-mobility, the feasible base locations consists of a region on the x-axis the boundaries of which are derived in the paper. The results are used to obtain the base locations so that the robot can reach a vertical line, a square surface, and a cubic volume. Two practical applications of the method at the JPL Surface Inspection Laboratory are described: scanning a surface and reaching inside an opening. The results of the paper are extended to mobile robots with two and three degrees-of-mobility.

1 Introduction

In performing various routine tasks such as wiping a table or cleaning a window, the human moves his body in order to position his arm in a comfortable configuration. For manipulator arms, there are numerous applications in which the mobility of the manipulator base is essential for successful execution of the task. An example of such mobile manipulators is the robotic system planned by NASA for the Space Station Freedom. In this system, the Special Purpose Dexterous Manipulator (SPDM) operates from the end of the Space Station Remote Manipulator System (SSRMS). The SSRMS is a crane arm which has a large work envelope, slow movement characteristics, a high payload handling capacity, and is used as a crude positioning device. The SPDM, on the other hand, is a smaller and lighter manipulator that can provide dexterous manipulation with fast and precise movement capability. A terrestrial application of mobile manipulators can be found in the DOE Waste Management Program at Hanford site. In this case, a large SPAR arm is used as the base positioner for a small Schilling arm that carries sensors to characterize the contents of an underground waste storage tank.

In mobile manipulators, such as the two examples cited above, proper placement of the manipulator base is *crucial* for successful execution of the task. At the present time, base

placement is done manually by the operator based on visual data obtained from the work-site. This approach is prone to error due to potential misjudgement of the operator, and is time consuming because of the trial-and-error search procedure involved. Furthermore, in worksites where viewing is hard or impossible, visual base placement is totally inadequate. It is, therefore, highly desirable to implement automated base placement methods to improve the efficiency of the system significantly. Several researchers have studied the kinematic and dynamic interactions between the mobile platform and the manipulator arm, and have proposed methods for coordinating the base mobility with the arm manipulation [1-8]. Most of the proposed methods address *on-line* coordination of mobility and manipulation in which the base and the arm move simultaneously to accomplish user-defined tasks. In many applications, such as in the Space Station Freedom, simultaneous motion of the base and the arm is *not* allowed due to operational constraints, added control complexity, safety and reliability considerations, and so on. In such applications, the base mobility must be activated initially to properly position the arm for task execution, and the base must remain immobile during the execution of the task by the arm. Therefore, the base is merely a positioner for the arm, rather than an active degree-of-freedom during task execution. This *off-line* approach to base placement leads to a simpler control scheme, since the base and the arm are not moved simultaneously, and is operationally simpler, more reliable, and safer. This paper presents a simple off-line method for base placement in mobile manipulators. The method utilizes "arm reachability" as the basic criterion for base placement to ensure that the target is within comfortable reach of the arm, and undesirable over-extended or under-extended arm configurations are avoided.

The paper is organized as follows. Section 2 describes base placement for target point reachability and presents a sensitivity analysis. The results are extended in Section 3 to determine base placement to scan a given line, surface, or volume. Section 4 describes two applications from a laboratory setup at JPL to demonstrate base placement to scan a surface or reach inside an opening. The foregoing results on 1D base motion are extended to 2D and 3D mobile bases in Section 5. Section 6 highlights the key features of the method and draws some conclusions.

2 Base Placement for Target Point Reachability

In this section, we derive the conditions under which a robot manipulator mounted on a mobile platform can reach a target point. Mobile platforms can assume different forms and three typical examples are depicted in Figure 1, showing a tracked robot with one degree-of-mobility, a wheeled robot with two degrees-of-mobility, and a gantry robot with three degrees-of-mobility. In this paper, it is assumed initially that the base mobility is a translational motion in one Cartesian direction such as the robot mounted on track in Figure 1; however, extensions to 2D and 3D base motions will be presented in Section 5. The robot manipulators considered in this paper are spatial arms capable of positioning the hand in the three-dimensional Cartesian work space. Typical examples of such robots are a three-jointed

non-redundant arm such as PUMA or a four-jointed redundant arm such as the Robotics Research Corporation arm. No consideration is given to the hand orientation, since we are only concerned with the placement of the hand frame origin on the target.

Figure 2 depicts the system under study, showing a robot arm mounted on a mobile platform in the three-dimensional task space. The fixed world coordinate frame-of-reference \mathcal{W} is defined such that the base translational motion is along the x-axis (in the positive or negative directions) and the robot shoulder has zero z-coordinate. This particular choice of the world frame simplifies the analysis considerably; hence when the task coordinates are expressed relative to any other world frame, they are transferred initially to the world frame \mathcal{W} before the analysis. For the sake of generality, the arm is assumed to have four joint degrees-of-freedom consisting of the shoulder roll and pitch (θ_1, θ_2) and elbow roll and pitch (θ_3, θ_4), thus emulating a redundant Robotics Research arm. The extra degree-of-freedom (i.e., redundancy) allows the elbow E to move out of the vertical plane passing through the shoulder S and the wrist W; thus enabling reconfiguration of the arm without perturbing the wrist position. This feature is, however, irrelevant to the reachability analysis presented in this section since it does not have any effect on the wrist position. The upper-arm SE and the forearm EW have the lengths l_1 and l_2 respectively. The angle between the upper-arm and forearm SEW is defined as the "elbow angle" ϕ . Notice that the elbow angle ϕ is completely independent of the arm angle ψ between the arm plane SEW and the reference vertical plane passing through SW; hence ϕ is unaltered when the arm is executing a self-motion where W is fixed and E traverses a circle around SW (the radius of the self-motion circle is a function of the elbow angle).

Before addressing the problem of base placement to reach a target point, let us investigate the workspace boundaries of the mobile robot. For this purpose, we first consider the "reach" of the arm. By applying the law of cosines to the SEW triangle, we obtain

$$r^2 = l_1^2 + l_2^2 - 2l_1l_2\cos\phi \quad (1)$$

where $r = SW$ is the shoulder-wrist distance, hereafter referred to as the "reach" of the arm. Notice that from equation (1) the arm reach r is only a function of the elbow angle ϕ . In the common case where the upper-arm and forearm are of equal length, such as in PUMA and Robotics Research arms, $l_1 = l_2 = l$ and equation (1) simplifies to

$$r^2 = 2l^2(1 - \cos\phi) = 4l^2\sin^2\frac{\phi}{2} \rightarrow r = 2l\sin\frac{\phi}{2} \quad (2)$$

Hence the arm reach r is a simple sinusoidal function of the elbow angle ϕ . From equation (1), it is seen that when ϕ changes in the range $0 \leq \phi \leq 180^\circ$, r varies from $|l_1 - l_2|$ to $l_1 + l_2$, with $r_{min} = |l_1 - l_2|$ at $\phi = 0$ (arm fully folded) and $r_{max} = l_1 + l_2$ at $\phi = 180^\circ$ (arm fully extended). Therefore, for a fixed base platform location, the reachable workspace of the arm is the space confined between two concentric spheres with center at $(\alpha, 0, 0)$ and radii r_{min} and r_{max} , where $x = \alpha$ is the base location. As the base platform moves along the x-axis, these two spheres sweep two coaxial cylinders which share the x-axis and have radii

r_{min} and r_{max} . Note that at end-of-travel of the platform on either side α_{min} and α_{max} , the cylinders are "capped" with hemispheres with centers at extreme base locations. Figure 3 shows the reachable workspace of the mobile robot when the elbow angle ϕ is unconstrained. For any target point in the reachable workspace shown in Figure 3, there is a corresponding base position α and arm angle ϕ for which the wrist will reach the target. Any point which lies outside the shaded space is unreachable by the arm.

When the user defines "preferred" configurations of the arm by restricting the elbow angle as $\phi_{min} \leq \phi \leq \phi_{max}$, where $\phi_{min} > 0$ and $\phi_{max} < 180^\circ$, the size of the reachable workspace reduces while its general shape is retained. In this case, the reachable workspace of the arm will be a hollow capsule-like space as shown in Figure 3 with r_{min} and r_{max} computed from:

$$r_{min} = [l_1^2 + l_2^2 - 2l_1l_2\cos\phi_{min}]^{\frac{1}{2}} ; r_{max} = [l_1^2 + l_2^2 - 2l_1l_2\cos\phi_{max}]^{\frac{1}{2}} \quad (3)$$

Again, in the common case when $l_1 = l_2 = l$, equation (3) reduces to

$$r_{min} = 2l\sin\frac{\phi_{min}}{2} ; r_{max} = 2l\sin\frac{\phi_{max}}{2} \quad (4)$$

Now, let us denote the target point in the task-space by $T(X, Y, Z)$, where the constant Cartesian coordinates X, Y , and Z are measured relative to the world frame \mathcal{W} . Then, the condition for reachability of the target point T by the arm is that T lies in the reachable workspace shown in Figure 3. For an unconstrained elbow angle (i.e., $0 \leq \phi \leq 180^\circ$), this requires

$$|l_1 - l_2| \leq D \leq l_1 + l_2 \quad (5)$$

where $D = [Y^2 + Z^2]^{\frac{1}{2}}$ is the distance of T from the x-axis. For the constrained elbow angle (i.e., $\phi_{min} \leq \phi \leq \phi_{max}$), the reachability condition becomes

$$r_{min} \leq D \leq r_{max} \quad (6)$$

where r_{min} and r_{max} are defined in equation (3). Note that in the common case $l_1 = l_2 = l$, equations (5) and (6) simplify to

$$D \leq 2l \quad ; \quad \left[2l\sin\frac{\phi_{min}}{2} \right] \leq D \leq \left[2l\sin\frac{\phi_{max}}{2} \right] \quad (7)$$

respectively.

Now, we turn to the problem of base placement for a reachable target point. Let the position of the base platform be represented by the shoulder coordinate $S(\alpha, 0, 0)$ and the target point be denoted by $T(X, Y, Z)$, both in the world frame \mathcal{W} . Then, for the wrist W to coincide with the target point T , the following two relationships must hold simultaneously:

$$(X - \alpha)^2 + Y^2 + Z^2 = r^2 \quad (8)$$

$$r^2 = l_1^2 + l_2^2 - 2l_1l_2\cos\phi \quad (9)$$

where equation (8) is the Euclidian distance between the shoulder S (α , 0, 0) and target T(X, Y, Z). Equations (8) and (9) represent the fundamental relationships between the base location α and the elbow angle ϕ , for a given target position T. Equating (8) and (9), we obtain

$$(X - \alpha)^2 = l_1^2 + l_2^2 - Y^2 - Z^2 - 2l_1l_2\cos\phi = \rho^2 \quad (10)$$

where ρ is only a function of ϕ , given Y and Z. Given the desired elbow angle ϕ , equation (10) gives two solutions for the base location α as

$$\alpha = X \pm \rho \quad (11)$$

The "right" solution $\alpha_r = X + \rho$ and the "left" solution $\alpha_l = X - \rho$ are symmetrical about the center point $\alpha_c = X$, as expected from the task geometry.

Now, given the target point T(X, Y, Z), the base location for which the elbow angle is at its minimum is given by $\alpha_c = X$, i.e., the base right in front of the target, and the minimum elbow angle ϕ_m is found from (10) as

$$\phi_m = \cos^{-1} \left[\frac{l_1^2 + l_2^2 - D^2}{2l_1l_2} \right] \quad (12)$$

As the base moves away from $\alpha_c = X$ in either direction, the elbow angle increases and ultimately reaches 180° when the arm becomes fully extended. The extreme base locations α_m for $\phi = 180^\circ$ are found from (10) as

$$\alpha_m = X \pm [(l_1 + l_2)^2 - D^2]^{\frac{1}{2}} \quad (13)$$

Figure 4 shows the region of feasible base locations on the x-axis from which the target point T is reachable by the arm. The region is centered at $\alpha_c = X$ and is composed of a right region extending to $\alpha_{mr} = X + [(l_1 + l_2)^2 - D^2]^{\frac{1}{2}}$, and a left region extending to $\alpha_{ml} = X - [(l_1 + l_2)^2 - D^2]^{\frac{1}{2}}$. Notice that the region is continuous and its width is given by $\Delta = 2[(l_1 + l_2)^2 - D^2]^{\frac{1}{2}}$. Therefore, the feasible base locations are given by

$$X - [(l_1 + l_2)^2 - D^2]^{\frac{1}{2}} \leq \alpha \leq X + [(l_1 + l_2)^2 - D^2]^{\frac{1}{2}} \quad (14)$$

Note: When the allowable range of elbow angle is specified as $\phi_{min} \leq \phi \leq \phi_{max}$, with $\phi_{min} > \phi_m$ and $\phi_{max} < 180^\circ$, then only *portions* of the region shown in Figure 4 are useable, and the continuity of the region is lost. The two extremes of the allowable right and left portions are found from equation (10) as

$$\alpha_{min} = X \pm [l_1^2 + l_2^2 - D^2 - 2l_1l_2\cos\phi_{min}]^{\frac{1}{2}}; \alpha_{max} = X \pm [l_1^2 + l_2^2 - D^2 - 2l_1l_2\cos\phi_{max}]^{\frac{1}{2}} \quad (15)$$

Note that the portions are symmetrical about the center point $\alpha_c = X$.

Finally, let $T = \{T_1, T_2, \dots, T_n\}$ be a set of n randomly positioned target points in the robot workspace. Then the common base location from which the mobile robot can reach the entire set T is given by the intersection of the feasible regions $\alpha = \{\cap \alpha_i\}$, where α_i is the allowable base region for the target point T_i . Note that when α is a null set, there is no base location for the robot to reach the entire set T .

Sensitivity Analysis: Given a fixed target point $T(X, Y, Z)$, we now find the sensitivity of ϕ to α , that is, the relationship between perturbation in base position $\delta\alpha$ and the corresponding change in the elbow angle $\delta\phi$. Consider the basic equation relating α to ϕ , that is

$$(X - \alpha)^2 + Y^2 + Z^2 = l_1^2 + l_2^2 - 2l_1l_2\cos\phi$$

Taking derivatives on both sides yields

$$-2(X - \alpha)\delta\alpha = 2l_1l_2\sin\phi\delta\phi$$

Assuming $\sin\phi \neq 0$, i.e., $\phi \neq 0, 180^\circ$, we obtain

$$\delta\phi = \frac{\alpha - X}{l_1l_2\sin\phi} \rightarrow \frac{\delta\phi}{\delta\alpha} = \frac{\alpha - X}{l_1l_2\sin\phi} \quad (16)$$

It is seen that the larger the upper-arm and forearm lengths l_1 and l_2 , the smaller will be the effect of base displacement $\delta\alpha$ on the elbow angle change $\delta\phi$, as expected, i.e., the less will be the sensitivity of ϕ to changes in α .

3 Base Placement to Reach a Target Line, Surface, and Volume

In this section, the results developed in the previous section will be used in three typical applications to find the proper base placement for the arm to reach a target line, a target surface, and a target volume in the workspace.

3.1 Reaching a Target Line

Suppose that we wish to place the robot base in order to reach the line passing through the points T_1, \dots, T_n . For simplicity, we assume that the line to be reached is a straight-line perpendicular to the x-y plane, as shown in Figure 5. First, consider the target point $T_1(X, Y, Z)$. Following Section 2, we can find the region on the x-axis for feasible base location to reach T_1 . Now, since the base calculations depend only on the distance of T_1 to the x-axis, $D = [Y^2 + Z^2]^{\frac{1}{2}}$, the mirror image of T_1 relative to the x-y plane yields exactly the same base locations. Therefore, we only need to consider the top (above x-y plane) or the bottom portion of the line $T_1 T_n$, whichever is *longer*.

Suppose that we take the top portion T_1, \dots, T_m , where T_m is the intersection of the $T_1 T_n$ line with the x-y plane. Then, as we move down from T_1 toward T_m , the distance to the x-axis (namely D) decreases since z decreases. Hence the minimum elbow angle ϕ_m defined in Section 2 decreases. The smallest value of ϕ_m occurs at the point T_m , since $z = 0$ and hence $D = y$ is at its minimum. Furthermore, as D decreases, the base extreme positions α_{ml} and α_{mr} and the width of the feasible region Δ defined in Section 2 all increase. Hence, for T_m we obtain the smallest ϕ_m , the largest feasible region Δ and the farthest extreme base locations α_{ml} and α_{mr} . Conversely, for T_1 we obtain the largest ϕ_m , the smallest feasible region Δ and the nearest extreme base locations α_{ml} and α_{mr} . Therefore, the feasible base locations to reach the entire line $T_1 T_n$ is clearly defined by the base locations for T_1 .

In the above discussions, we assumed that the elbow angle ϕ is not restricted by the user and "absolute reachability" of the arm is considered. The user can restrict the elbow angle as $\phi_{min} \leq \phi \leq \phi_{max}$, with $\phi_{min} > \phi_m$ and $\phi_{max} < 180^\circ$, to avoid undesirable over-extended or under-extended arm configurations. Under this "preferred reachability" restriction, the allowable base locations are a subset of those obtained with unrestricted elbow angle. When $\phi_{min} \leq \phi \leq \phi_{max}$, we first find the allowable left and right regions $\alpha_{1l} = \{\alpha_{min,l} \leq \alpha \leq \alpha_{max,l}\}_{T_1}$ and $\alpha_{1r} = \{\alpha_{min,r} \leq \alpha \leq \alpha_{max,r}\}_{T_1}$ on the x-axis to reach the point T_1 . The procedure is then repeated for the point T_m to find the left and right regions $\alpha_{ml} = \{\alpha_{min,l} \leq \alpha \leq \alpha_{max,l}\}_{T_m}$ and $\alpha_{mr} = \{\alpha_{min,r} \leq \alpha \leq \alpha_{max,r}\}_{T_m}$. The overlap between these sets, namely

$$\alpha_l = \alpha_{1l} \cap \alpha_{ml} ; \alpha_r = \alpha_{1r} \cap \alpha_{mr} \quad (17)$$

gives the left and right regions for base placement on the x-axis to reach the entire line $T_1 T_n$.

The method is illustrated by a numerical example in Section 4.1.

3.2 Reaching a Target Surface

In this section, we use the results of Section 3.1 to determine the proper base location when the robot is required to reach a target square surface. It is reasonable to assume that the target surface is oriented parallel to the x-axis, since the base platform translation is usually installed so that the arm can reach an extended surface by activating the base motion.

The surface reach analysis is based on the fact that the base location α is a *linear* function of the x-coordinate of the target point X . This is in contrast to dependence of α on Y and Z which is nonlinear. The linearity of the (α, X) relationship implies that when the target point $T(X, Y, Z)$ is shifted in the x-direction by the amount δ to $S(X + \delta, Y, Z)$, then the feasible region of base locations for S is obtained by shifting the region for T by the same amount δ .

Now, suppose that the line $T_1 T_n$ is shifted to the right in the x-direction by the amount δ to the line $S_1 S_n$ to generate the rectangle $T_1 S_1 S_n T_n$ as shown in Figure 6. For the line $T_1 T_n$, using Section 3.1, the feasible base locations are found to be a region with center at $\alpha_c = X$ and extremes α_{ml} and α_{mr} , and width Δ , see Figure 6. Now, as the line $T_1 T_n$ moves

parallel to itself to the right by δ to sweep the area $T_1 S_1 S_n T_n$, the base moves by the same amount δ , since the governing equations are linear in X . Hence for the line $S_1 S_n$, the region is obtained by shifting by δ the region for $T_1 T_n$, and is shown as cross-hatched in Figure 6. The overlap between the two regions $\{\alpha_{ml} \leq \alpha \leq \alpha_{mr}\}$ for $T_1 T_n$ and $\{\alpha_{ml} + \delta \leq \alpha \leq \alpha_{mr} + \delta\}$ for $S_1 S_n$ defines the feasible locations for the base platform for the arm to be able to reach the entire surface $T_1 S_1 S_n T_n$. Now, the *maximum* value of δ for which the two regions for $T_1 T_n$ and $S_1 S_n$ have an overlap is given by $\delta_{max} = \Delta$, in which case the common region reduces to a single point α_{mr} . We conclude that the *maximum* size of the rectangle $T_1 S_1 S_n T_n$ reachable by a *fixed* base location is Δ . Therefore, an extended surface needs to be segmented into rectangles with maximum width Δ , and for each segment there will be an appropriate base location from which the arm can reach the entire segment.

In the above analysis, we only considered the shift of the line $T_1 T_n$ in one direction, i.e., to the right. By a similar argument, when the line $T_1 T_n$ is shifted to the left by the amount δ to the line $R_1 R_n$, the region of feasible base locations $\{\alpha_{ml} \leq \alpha \leq \alpha_{mr}\}$ is displaced by $-\delta$ to $\{\alpha_{ml} - \delta \leq \alpha \leq \alpha_{mr} - \delta\}$. Therefore, when base motion to both right and left directions is allowed, the overlap of the three regions: $\{\alpha_{ml} - \delta \leq \alpha \leq \alpha_{mr} - \delta\}$, $\{\alpha_{ml} \leq \alpha \leq \alpha_{mr}\}$ and $\{\alpha_{ml} + \delta \leq \alpha \leq \alpha_{mr} + \delta\}$, defines the feasible base locations to reach the entire surface $R_1 T_1 S_1 S_n T_n R_n$. In this case, the maximum value of δ for which the three regions have an overlap is $\delta_{max} = \frac{\Delta}{2}$, in which case the common band reduces to a single joint $\alpha_c = X$. Therefore, the *maximum* size of the rectangle $R_1 S_1 S_n R_n$ reachable by a *fixed* base location is again $2\delta_{max} = \Delta$, as in the previous case. Note that, however, in this case the base location is on the center line of the scanned rectangle.

3.3 Reaching a Target Volume

In this section, we discuss the placement of base in order to scan a target cubic volume $S_1 T_1 U_1 V_1 V_n S_n T_n U_n$, as shown in Figure 7. Let us start with the line $T_1 T_n$. Following Section 3.1, we find the region on the x-axis of feasible base locations for reaching the line $T_1 T_n$. This region is centered at $\alpha_c = X$ and extends from α_{ml} to α_{mr} , i.e., $\{\alpha_{ml} \leq \alpha \leq \alpha_{mr}\}$, (see Figure 7). Now, suppose that the line $T_1 T_n$ is moved parallel to itself in the y-direction to $U_1 U_n$. Then, following Section 3.1, we find the feasible base locations $\{\alpha'_{ml} \leq \alpha \leq \alpha'_{mr}\}$ with center at α'_c and width $\Delta' = \alpha'_{mr} - \alpha'_{ml}$ from which the wrist can reach $U_1 U_n$ with $\phi_m \leq \phi \leq 180^\circ$. This will be a smaller region than for $T_1 T_n$ (since the y-coordinates are larger), and, therefore, the overlap between the regions for $T_1 T_n$ and $U_1 U_n$ is clearly the region for $U_1 U_n$ as shown in Figure 7. Therefore, if the base is placed in the region $\{\alpha'_{ml} \leq \alpha \leq \alpha'_{mr}\}$, the wrist can reach every point on the surface $T_1 U_1 U_n T_n$.

Now, the rectangular cube $S_1 T_1 U_1 V_1 V_n S_n T_n U_n$ is generated by moving the surface $T_1 U_1 U_n T_n$ parallel to itself in the x-direction by the amount $\delta = T_1 S_1$. Since the dependency of the base location α on the x-coordinate is *linear*, the feasible region for the surface $S_1 V_1 V_n S_n$ is obtained by shifting the base region for $T_1 U_1 U_n T_n$ by the amount δ . Clearly, for the two regions to have an overlap, we require $\delta \leq \Delta$, where Δ is the width of the feasible region for

reaching $T_1 U_1 U_n T_n$. Assuming $\delta \leq \Delta$, then any point on the overlap of $\{\alpha_{ml} \leq \alpha \leq \alpha_{mr}\}$ and $\{\alpha_{ml} + \delta \leq \alpha \leq \alpha_{mr} + \delta\}$ is a feasible base location for reaching the entire cube $S_1 T_1 U_1 V_1 V_n S_n T_n U_n$. Notice that when $T_1 S_1 > \Delta$, we first need to segment the cube into smaller cubic slices with maximum width Δ , and then find the proper base placement for each slice.

4 Practical Applications

In this section, we describe two practical applications of the foregoing analysis in the JPL Surface Inspection Laboratory. The Laboratory setup is shown in Figure 8 and consists of a 7 DOF Robotics Research Arm mounted on a motorized platform with one degree of translational mobility and a 1/3 scale mockup of a truss structure that emulates part of the Space Station Freedom. The arm is carrying sensors at its end-effector for inspection of both the external and internal surfaces of the truss. Since the analysis deals with positioning of the wrist center, only the first four joints on the arm, namely shoulder roll/pitch and elbow roll/pitch, are considered. Note that there is a redundant joint in the arm for the control of three wrist Cartesian coordinates, and this redundancy allows the elbow to rotate around the shoulder-wrist line without perturbing the wrist position and thus provides the capability for arm reconfiguration.

Figure 9 shows the schematic of the experimental setup. The Robotics Research Arm is approximated by two thin uniform rods with equal lengths $l_1 = l_2 = l = 67$ cm representing the upper-arm and the forearm, and the joint offsets are ignored. The world coordinate frame of reference used in the laboratory is denoted by \mathcal{W} in Figure 9. For the purpose of our analysis, we will use the world frame \mathcal{W} as defined in Figure 9 in which the z-coordinate of the shoulder is zero. In order to deal with the wrist center, we allow for the sensor length of 10 cm and the standoff distance of 20 cm (distance between truss and sensor) in our analysis and project the truss structure by 30 cm in the negative y-direction to obtain the "fake" truss shown in Figure 9.

Two practical applications are considered in this section. In the first application, we wish to find the location of the base platform so that the hand-mounted sensors can scan the surface of an Orbital Replacement Unit (ORU) mounted on the truss. In the second application, we need to determine the platform position to enable the sensor to reach inside a truss opening.

4.1 Surface Scan

In this application, we wish to scan the surface of the rectangle ABCD shown in Figure 9, where the vertices have the following coordinates in the world frame \mathcal{W} :

$$A = \begin{cases} x = 309 \\ y = 55 \\ z = 47 \end{cases} ; B = \begin{cases} x = 396 \\ y = 55 \\ z = 47 \end{cases} ; C = \begin{cases} x = 396 \\ y = 55 \\ z = -19 \end{cases} ; D = \begin{cases} x = 309 \\ y = 55 \\ z = -19 \end{cases}$$

and the unit of length is centimeter. First, we consider the line AD. We notice that $|A| > |D|$, and therefore from Section 3.1 we only need to consider the point A which is the farthest point on the line AD from the x-axis. For point A, we find the region of feasible base locations on the x-axis from which the wrist can reach A. Following Section 3.1, when the base is positioned at $\alpha_c = X_A = 309$, the elbow angle is found as

$$\phi_m = \cos^{-1} \left[\frac{l_1^2 + l_2^2 - Y_A^2 - Z_A^2}{2l_1l_2} \right] = \cos^{-1}(0.417) = 65.35^\circ$$

As the base moves away from α_c , the elbow angle increases and ultimately reaches 180° when the base is at

$$\alpha_m = X_A \pm [(l_1 + l_2)^2 - Y_A^2 - Z_A^2]^{\frac{1}{2}} = 309 \pm 112.8 = 421.8, 196.2 \text{ cm}$$

Therefore, the feasible region for the line AD consists of a segment of the x-axis extending from $\alpha_{ml} = 196.2$ to $\alpha_{mr} = 421.8$ with center at $\alpha_c = 309$ and width $\Delta = 225.6$ cm. Now, we need to find out the smallest elbow angle when the wrist is scanning the line AD. Consider the point $P[x = 309, y = 55, z = 0]$ where the line AD crosses the x-y plane. When the base is placed at α_c and α_{ml} , the elbow angles for P are found as:

$$\alpha = \alpha_c \quad \phi = 48.47^\circ \quad ; \quad \alpha = \alpha_{mr} \quad \phi = 138.94^\circ$$

We conclude that when the base is at the center point α_c , all points on the line AD can be reached with the elbow angle in the range $48.47^\circ \leq \phi \leq 65.35^\circ$. When the base is at the extreme points α_{mr} or α_{ml} , the elbow angle range is $138.94^\circ \leq \phi \leq 180^\circ$.

Now, as the line AD sweeps the area ABCD to reach the line BC, the feasible region shifts by the amount $\delta = X_B - X_A = 87$ cm in the x-direction. Hence, the feasible region for the line BC is given by $\{\alpha_{ml} + \delta \leq \alpha \leq \alpha_{mr} + \delta\} = \{283.2 \leq \alpha \leq 508.8\}$. Therefore, the overlap between the reachable regions for AD and BC is found to be

$$283.2 \leq \alpha \leq 421.8$$

For instance, we can choose the midpoint of this region and place the base platform at $\alpha = 352.5$ cm [which corresponds to the middle of rectangle ABCD] to reach the entire ABCD surface.

Let us now re-examine the problem when the elbow angle is restricted to lie in the range $70^\circ \leq \phi \leq 150^\circ$ defined by the user. In this case, at the lower bound $\phi = 70^\circ$, for the points A and P we have

$$\text{Point A: } \alpha = X_A \pm [l_1^2 + l_2^2 - Y_A^2 - Z_A^2 - 2l_1l_2\cos\phi]^{\frac{1}{2}} = 309 \pm 26.3 = 282.7, 335.3 \text{ cm}$$

$$\text{Point P: } \alpha = X_P \pm [l_1^2 + l_2^2 - Y_P^2 - Z_P^2 - 2l_1l_2\cos\phi]^{\frac{1}{2}} = 309 \pm 53.9 = 255.1, 362.9 \text{ cm}$$

Note that there are two solutions for each point corresponding to the right and left of the center point α_c . Similarly, at the upper bound $\phi = 150^\circ$, the left and right solutions for each point are found as

$$\text{Point A: } \alpha = 309 \pm 107.5 = 201.5, 416.5 \text{ cm}$$

$$\text{Point P: } \alpha = 309 \pm 117.3 = 191.7, 426.3 \text{ cm}$$

Hence, the allowable left regions are $\{201.5 \leq \alpha \leq 282.7\}$ for A and $\{191.7 \leq \alpha \leq 255.1\}$ for P; and the allowable right regions are $\{335.3 \leq \alpha \leq 416.5\}$ and $\{362.9 \leq \alpha \leq 426.3\}$ for A and P, respectively. Therefore, the overlap between the regions for A and P defines the allowable region for the entire line AD as:

$$\text{left region } \{201.5 \leq \alpha \leq 255.1\} \quad ; \quad \text{right region } \{362.9 \leq \alpha \leq 416.5\}$$

Note that the two regions are symmetrical about the center point $\alpha_c = 309$ but are discontinuous, and the width of each region is equal to $\Delta = 53.6$ cm. Now, as AD moves to the right by δ to sweep the area ABCD, the feasible region is shifted by δ to the right. However, since the width of the square $AB = 87$ cm exceeds the width of the region $\Delta = 53.6$ cm, it is impossible to find a single base location from which the arm can scan the entire rectangle ABCD with the specified elbow angle constraint $70^\circ \leq \phi \leq 150^\circ$. In this case, it is necessary to segment ABCD vertically into two smaller rectangles such as AEFD and EBCF as shown in Figure 9, where E and F are the midpoints of AB and CD, respectively. This reduces the width of the rectangle by half to $\frac{87}{2} = 43.5$ cm which is smaller than Δ ; hence each new rectangle can be scanned from a single base location. To scan the rectangle AEFD, we find the overlap between the left region $\{201.5 \leq \alpha \leq 255.1\}$ for AD and the shifted region $\{245 \leq \alpha \leq 298.6\}$ for EF as $\{245 \leq \alpha \leq 255.1\}$. For instance, we can place the base at the midpoint of this region at $\alpha = 250$ cm to scan the rectangle AEFD. Similarly, for the rectangle EBCF, the feasible left region is found to be $\{288.5 \leq \alpha \leq 298.6\}$ and a feasible base location is $\alpha = 293.5$ cm.

In comparison with the previous case where the elbow angle is unrestricted, it is seen that restriction of the elbow angle by the user has resulted in a smaller allowable region for base location. This means that it is not possible to scan the entire rectangle ABCD from a single base position while restricting the elbow angle to $70^\circ \leq \phi \leq 150^\circ$. Notice that the imposition of the elbow angle restriction has also resulted in discontinuous right and left regions on the x-axis; as opposed to the continuous region obtained when ϕ is unrestricted. However, by restricting the elbow angle at the user's specification, undesirable over-extended or under-extended arm configurations are avoided.

4.2 Reach Inside Opening

In this application, we wish to place the base so that the arm can reach safely inside the triangular opening ACD in the truss as shown in Figure 9.

The point of entry of the arm into the truss is chosen to be the center Q of the triangle ACD with the coordinates $x = 328.8$, $y = 55$, $z = 1$, where Q is equidistant from the sides of ACD. As a rule for placement of the base platform, we require that the wrist W, the forearm midpoint M, and the elbow E be able to enter the truss at the center Q. For the wrist W, we have $l_1 = 67$ cm, $l_2 = 67$ cm and hence

$$\phi_m = \cos^{-1} \left[\frac{l_1^2 + l_2^2 - Y^2 - Z^2}{2l_1l_2} \right] = \cos^{-1}(0.663) = 48.47^\circ$$

$$\alpha_m = X \pm [(l_1 + l_2)^2 - Y^2 - Z^2]^{\frac{1}{2}} = 328.8 \pm 122.2 = 206.6, 451 \text{ cm}$$

Therefore, when the base is placed in the region $\{206.6 \leq \alpha \leq 451\}$, the wrist W can reach the center Q with the elbow angle in the range $\{48.47^\circ \leq \phi \leq 180^\circ\}$. Similarly, for the forearm midpoint M to enter the truss at the center Q, we have $l_1 = 67$ cm, $l_2 = \frac{67}{2} = 33.5$ cm and hence

$$\phi_m = \cos^{-1}(0.576) = 54.83^\circ ; \alpha_m = 328.8 \pm 84.1 = 244.7, 412.9 \text{ cm}$$

This means that the forearm midpoint M can reach the center Q [with $54.83^\circ \leq \phi \leq 180^\circ$] when the base position lies in the region $\{244.7 \leq \alpha \leq 412.9\}$. In a similar manner, when the elbow E is entering the truss at the center Q, we can set $l_1 = 67$ cm, $l_2 = 0$ and obtain

$$(X - \alpha)^2 + Y^2 + Z^2 = l_1^2$$

$$\alpha = X \pm [l_1^2 - Y^2 - Z^2]^{\frac{1}{2}} = 328.8 \pm 38.2 = 290.6, 367 \text{ cm}$$

Note that the allowable base region is now reduced to two single points, and the elbow angle is no longer relevant. The overlap between the three possible base locations considering reachability of the wrist, the forearm midpoint, and the elbow is clearly $\alpha = 290.6, 367$.

We conclude that there are two solutions for the base placement: one solution $\alpha = 290.6$ cm is to the left of the center Q ($x = 328.8$) and the other solution $\alpha = 367$ cm is to the right of Q, with both solutions symmetrical about Q.

5 Extensions to Two and Three-Dimensional Base Mobility

In the foregoing analysis, we assumed that the robot base has one degree-of-freedom for translational motion along the x-axis in the world frame \mathcal{W} . In this section, the results are extended to mobile robots with two and three-dimensional mobile bases.

5.1 Two-Dimensional Mobile Base

In this section, we consider mobile robots with base mobility in two Cartesian directions such as a robot arm mounted on a vehicle as shown in Figure 1. The fixed world frame of reference \mathcal{W} is chosen such that the base translational motions are along the x-axis and the y-axis. Let $S(\alpha, \beta, 0)$ denote the base location, where α and β denote the base x and y-coordinates in \mathcal{W} . Then the governing equation is

$$(X - \alpha)^2 + (Y - \beta)^2 + Z^2 = l_1^2 + l_2^2 - 2l_1l_2\cos\phi \quad (18)$$

where $T(X, Y, Z)$ denotes the target point and ϕ is the elbow angle. With the elbow angle restricted to the user-defined range $\phi_{min} \leq \phi \leq \phi_{max}$, the reachable workspace of the mobile robot is given by

$$[l_1^2 + l_2^2 - 2l_1l_2\cos\phi_{min}]^{\frac{1}{2}} \leq |Z| \leq [l_1^2 + l_2^2 - 2l_1l_2\cos\phi_{max}]^{\frac{1}{2}} \quad (19)$$

Equation (19) defines a portion of the workspace bounded by the two parallel horizontal planes $Z_{min} = [l_1^2 + l_2^2 - 2l_1l_2\cos\phi_{min}]^{\frac{1}{2}}$ and $Z_{max} = [l_1^2 + l_2^2 - 2l_1l_2\cos\phi_{max}]^{\frac{1}{2}}$, assuming no restrictions on α and β . In the case where $\phi_{min} = 0$ and $\phi_{max} = 180^\circ$, equation (19) gives $|l_1 - l_2| < |Z| \leq (l_1 + l_2)$. Note that for a given target point $T(X, Y, Z)$, the smallest possible value of the elbow angle ϕ_m occurs when the base S is placed at $P(X, Y, 0)$, which is the projection of T onto the x-y plane. In this case, ϕ_m is obtained as

$$\phi_m = \cos^{-1} \left[\frac{l_1^2 + l_2^2 - Z^2}{2l_1l_2} \right] \quad (20)$$

Therefore, the unrestricted range of variation of the elbow angle to reach T is $\phi_m \leq \phi \leq 180^\circ$.

Now, for a given target point $T(X, Y, Z)$ and elbow angle ϕ , the loci of all possible base location $S(\alpha, \beta, 0)$ is defined by the circle

$$(\alpha - X)^2 + (\beta - Y)^2 = r^2 \quad (21)$$

where

$$r^2 = l_1^2 + l_2^2 - 2l_1l_2\cos\phi - Z^2 \quad (22)$$

In other words, the base S can be positioned anywhere on the circle centered at P with radius r . Now, as ϕ assumes values from ϕ_{min} to ϕ_{max} where $\phi_{min} \geq \phi_m$ and $\phi_{max} \leq 180^\circ$, the radius of the circle changes from $r_{min} = [l_1^2 + l_2^2 - 2l_1l_2\cos\phi_{min} - Z^2]^{\frac{1}{2}}$ to $r_{max} = [l_1^2 + l_2^2 - 2l_1l_2\cos\phi_{max} - Z^2]^{\frac{1}{2}}$. Therefore, we obtain a family of concentric circles with centers at P and radii in the range $r_{min} \leq r \leq r_{max}$, as shown in Figure 10. In other words, the allowable base location is a circular region in the x-y plane bounded by an inner circle with radius r_{min} and an outer circle with radius r_{max} , both centered at P . Note that when $\phi_{min} = \phi_m$ and $\phi_{max} = 180^\circ$, the radii of the inner and outer circles become $r_{min} = 0$ and $r_{max} = [(l_1 + l_2)^2 - Z^2]^{\frac{1}{2}}$,

respectively. Therefore, the allowable base location is the area of the circle centered at P with radius $[(l_1 + l_2)^2 - Z^2]^{\frac{1}{2}}$.

The allowable base region can also be obtained using a conceptually different approach. For the wrist W to reach the target point T(X, Y, Z), the base of the arm (i.e., the shoulder S) must be at a distance $d = [l_1^2 + l_2^2 - 2l_1l_2\cos\phi]^{\frac{1}{2}}$ from T, where ϕ is the elbow angle. The loci of all the points with distance d from T is a sphere with center at T and radius d. As the elbow angle changes from its minimum $\phi = 0^\circ$ to its maximum $\phi = 180^\circ$, d changes from $d_{min} = |l_1 - l_2|$ to $d_{max} = l_1 + l_2$. Therefore, we obtain a family of concentric spheres¹ centered at T with radii $|l_1 - l_2| \leq d \leq l_1 + l_2$. The smallest sphere which "touches" the x-y plane at point P(X, Y, 0) corresponds to the smallest elbow angle ϕ_m given by (20) for which the arm can just reach T. As ϕ is increased from ϕ_m to 180° , the intersections of the spheres with the x-y plane become a family of concentric circles centered at P, as shown in Figure 10. The largest circle which corresponds to $\phi = 180^\circ$ has radius $[(l_1 + l_2)^2 - Z^2]^{\frac{1}{2}}$. Therefore, for $\phi_m \leq \phi \leq 180^\circ$, the loci of all feasible base locations is the area of the circle centered at P(X, Y, 0) with radius $[(l_1 + l_2)^2 - Z^2]^{\frac{1}{2}}$. Notice that when ϕ is restricted by the user as $\phi_{min} \leq \phi \leq \phi_{max}$, the feasible base location becomes the annular region bounded by two circles centered at P with the inner circle radius $r_{min} = [l_1^2 + l_2^2 - 2l_1l_2\cos\phi_{min} - Z^2]^{\frac{1}{2}}$ and the outer circle radius $r_{max} = [l_1^2 + l_2^2 - 2l_1l_2\cos\phi_{max} - Z^2]^{\frac{1}{2}}$.

5.2 Three-Dimensional Mobile Base

In this section, mobile robots with base mobility in three Cartesian directions are considered, such as a robot arm mounted on an x-y-z gantry as shown in Figure 1.

Let S (α, β, γ) denote the base coordinates in the fixed world frame W chosen such that its axes coincide with the three base translational motions. Then, the wrist W will reach the target point T(X, Y, Z) provided that

$$(X - \alpha)^2 + (Y - \beta)^2 + (Z - \gamma)^2 = l_1^2 + l_2^2 - 2l_1l_2\cos\phi \quad (23)$$

In this case, if there are no restrictions on α, β , and γ , the arm can reach *all* points T in the workspace. Hence the reachable workspace is the entire three-dimensional task space.

For a given elbow angle ϕ and target point T, equation (23) gives

$$(\alpha - X)^2 + (\beta - Y)^2 + (\gamma - Z)^2 = r^2 \quad (24)$$

where

$$r^2 = l_1^2 + l_2^2 - 2l_1l_2\cos\phi \quad (25)$$

Equations (24) and (25) imply that the base can be positioned anywhere on the sphere with center at T(X, Y, Z) and radius r, which is a function of ϕ . When ϕ changes from 0 to 180° , we obtain a family of concentric spheres centered at T with radii ranging from $r_{min} = |l_1 - l_2|$

¹The results in Section 2 represent the intersections of the spheres with the x-axis.

to $r_{max} = l_1 + l_2$. Therefore, for a given target point T, the feasible base locations is the volume enclosed between two spheres centered at T with the inner radius $|l_1 - l_2|$ and the outer radius $l_1 + l_2$, as shown in Figure 11. Notice that when the elbow angle ϕ is restricted by the user to lie in the range $\phi_{min} \leq \phi \leq \phi_{max}$, then the feasible base locations consist of the volume enclosed between an inner sphere with radius $r_{min} = [l_1^2 + l_2^2 - 2l_1l_2\cos\phi_{min}]^{\frac{1}{2}}$ and an outer sphere with radius $r_{max} = [l_1^2 + l_2^2 - 2l_1l_2\cos\phi_{max}]^{\frac{1}{2}}$, both centered at T.

6 Conclusions

This paper addresses the problem of base placement for a mobile robot based on reachability analysis to accomplish a general task. An extremely simple and computationally efficient off-line method is presented for base placement. The method has been used in the JPL Surface Inspection Laboratory for two different applications: scanning a surface mounted on a truss and reaching inside an opening on the truss. The calculated positions have been verified as feasible base locations in the laboratory.

The analysis shows that for robots with 1D base mobility, the feasible base positions to reach a specified target point is a continuous region on the x-axis whose width is an inverse function of the distance between the target and the x-axis. For robots with 2D base mobility, the loci of feasible base positions is the area of a circle in the x-y plane whose radius is an inverse function of the distance between the target and the x-y plane. For robots with 3D base mobility, the feasible base location is the volume enclosed between two concentric spheres. The feasible base locations define possible ranges of values for the base coordinates from which the target can be reached. These inequity constraints, combined with additional user-defined constraints on the base coordinates, can be used to uniquely determine the base location to reach a specified target point. Future research will address the problem of imposing appropriate additional constraints to uniquely determine the "optimal" base location to execute a given task.

7 Acknowledgement

The research described in this paper was carried out at the Jet Propulsion Laboratory, California Institute of Technology, under contract with the National Aeronautics and Space Administration.

8 References

- [1] W.F. Carriker, P.K. Khosla, and B.H. Krogh: "An approach for coordinating mobility and manipulation," Proc. IEEE Conf. on Systems Engineering, August 1989.
- [2] W.F. Carriker, P.K. Khosla, and B.H. Krogh: "Path planning for mobile manipulators for multiple task execution," IEEE Trans. on Robotics and Automation, Vol. 7, No.3, pp.

403-408, June 1991.

- [3] W.F. Carriker, P.K. Khosla, and B.H. Krogh: "The use of simulated annealing to solve the mobile manipulator path planning problem," Proc. IEEE Conf. on Robotics and Automation, pp. 204-209, May 1990.
- [4] F.G. Pin and J.C. Culioli: "Optimal positioning of redundant manipulator - platform systems for maximum task efficiency," Proc. Intern. Symposium on Robotics and Manufacturing, pp. 489-495, July 1990.
- [5] F.G. Pin and J.C. Culioli: "Multi-criteria position and configuration optimization for redundant platform/manipulator systems," Proc. IEEE Workshop on Intelligent Robots and Systems, pp. 103-107, July 1990.
- [6] K. Liu and F.L. Lewis: "Decentralized continuous robust controller for mobile robots," Proc. IEEE Conf. on Robotics and Automation, pp. 1822-1827, May 1990.
- [7] N.A.M. Hootsmans and S. Dubowsky: "Large motion control of mobile manipulators including vehicle suspension characteristics," Proc. IEEE Conf. on Robotics and Automation, pp. 2336-2341, April 1991.
- [8] H. Seraji: "An on-line approach to coordinated mobility and manipulation," Proc. IEEE Conf. on Robotics and Automation, May 1993.

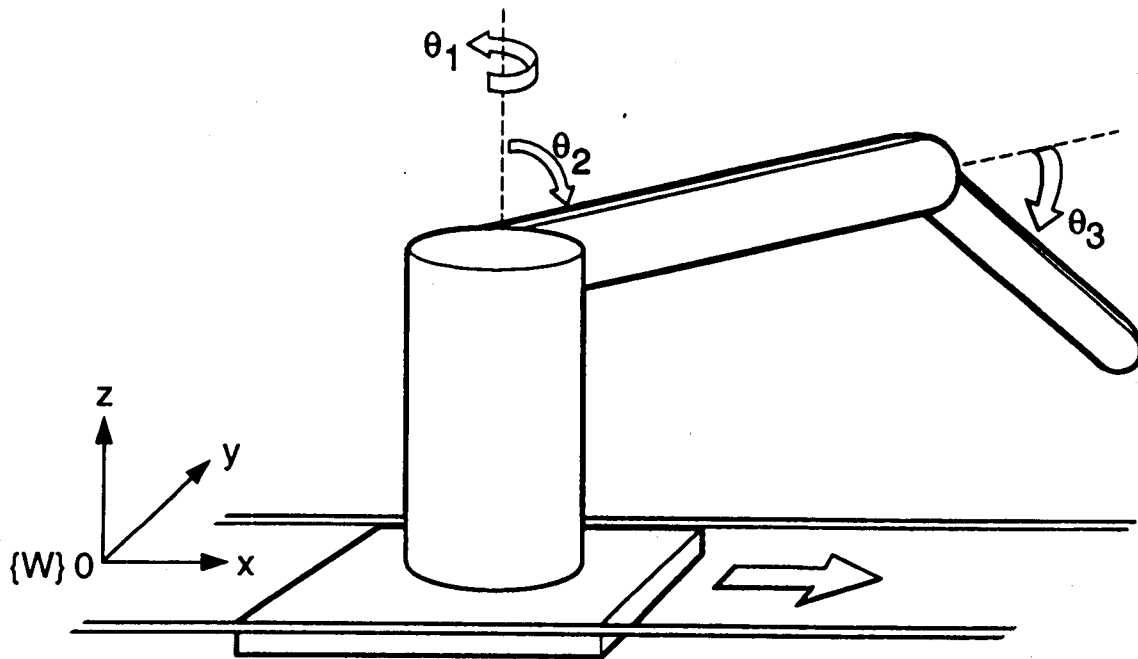


Figure 1a. Tracked robot

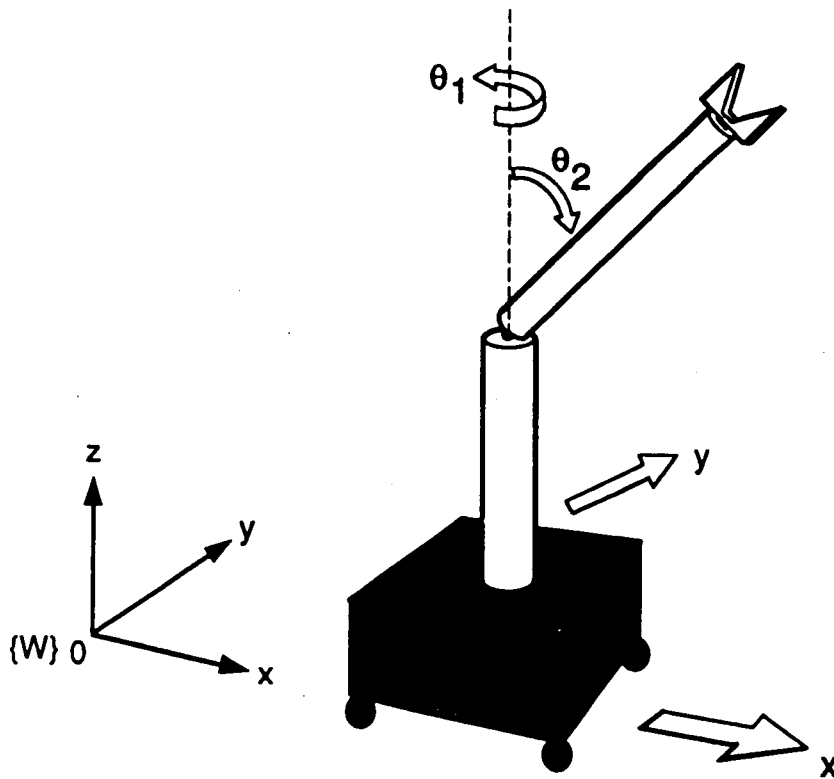


Figure 1b. Wheeled robot

Figure 1. Typical mobile robots

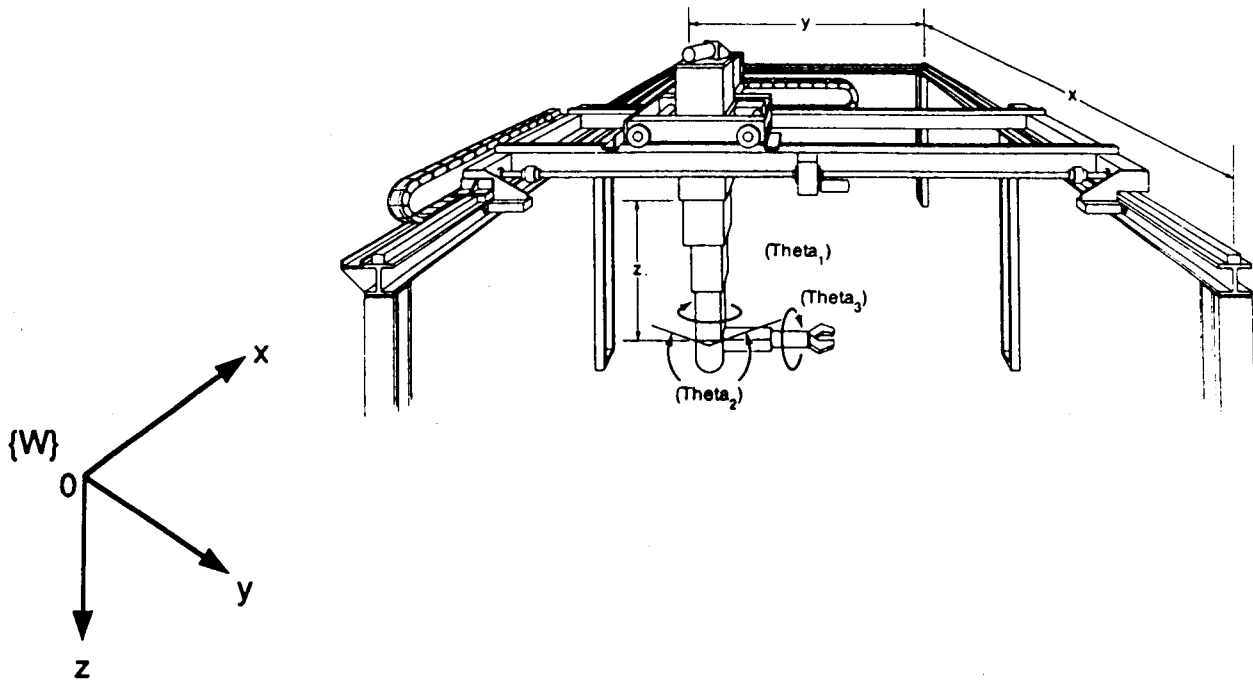


Figure 1c. Gantry robot

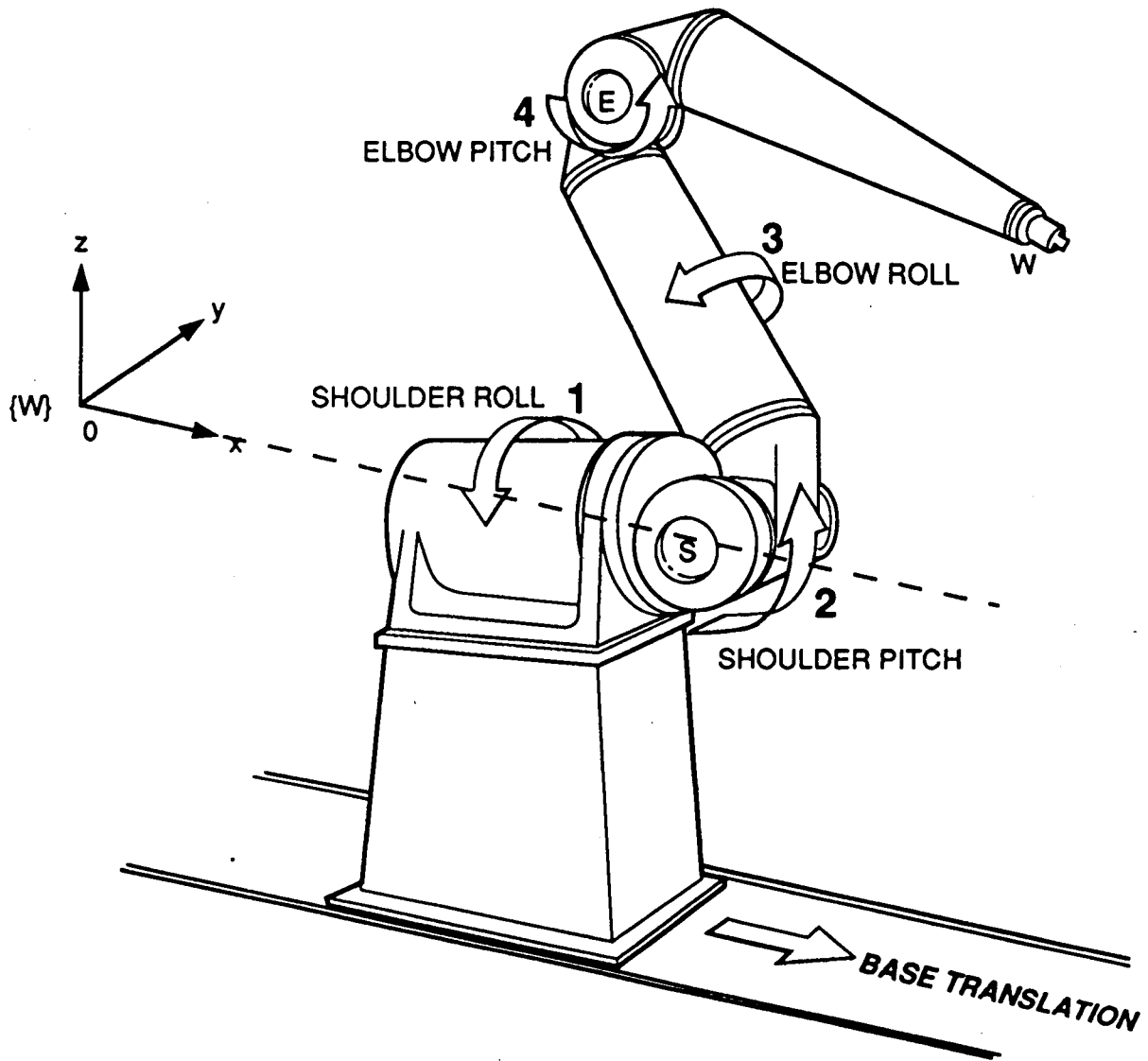


Figure 2. 4 DOF Robot arm mounted on 1 DOF mobile platform

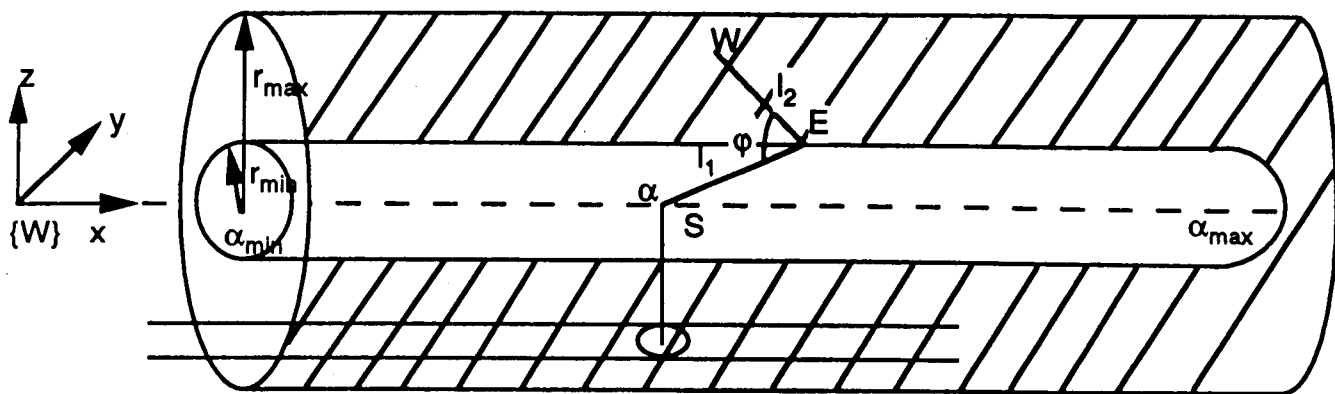


Figure 3. Reachable workspace of the mobile arm

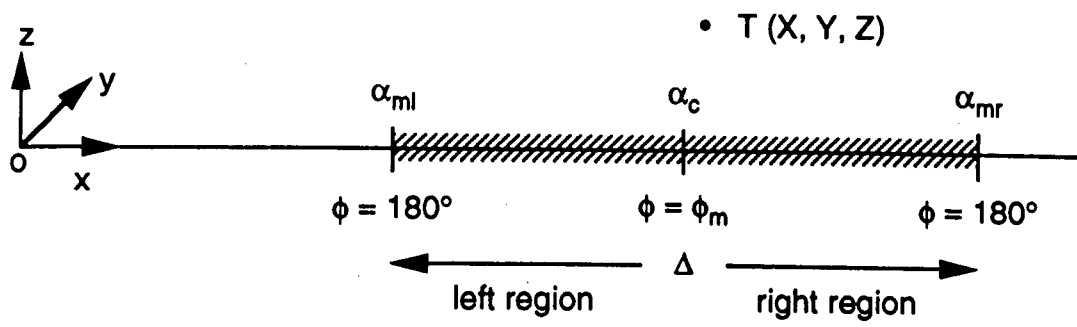


Figure 4. Feasible base locations to reach a point

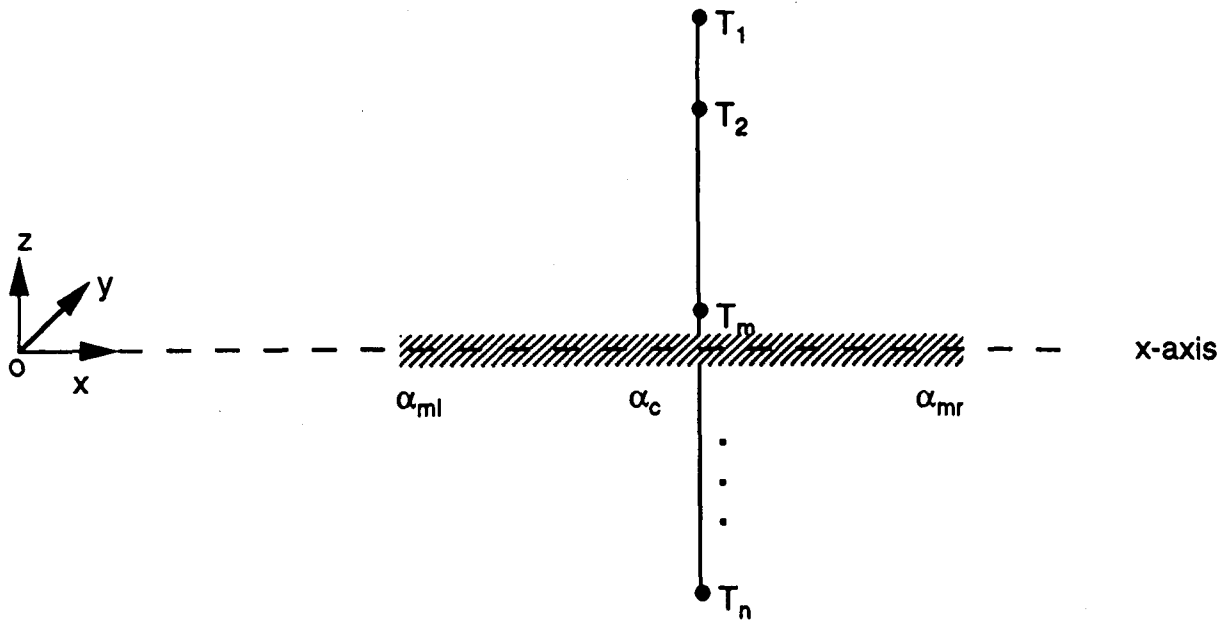


Figure 5. Feasible base locations to reach a line

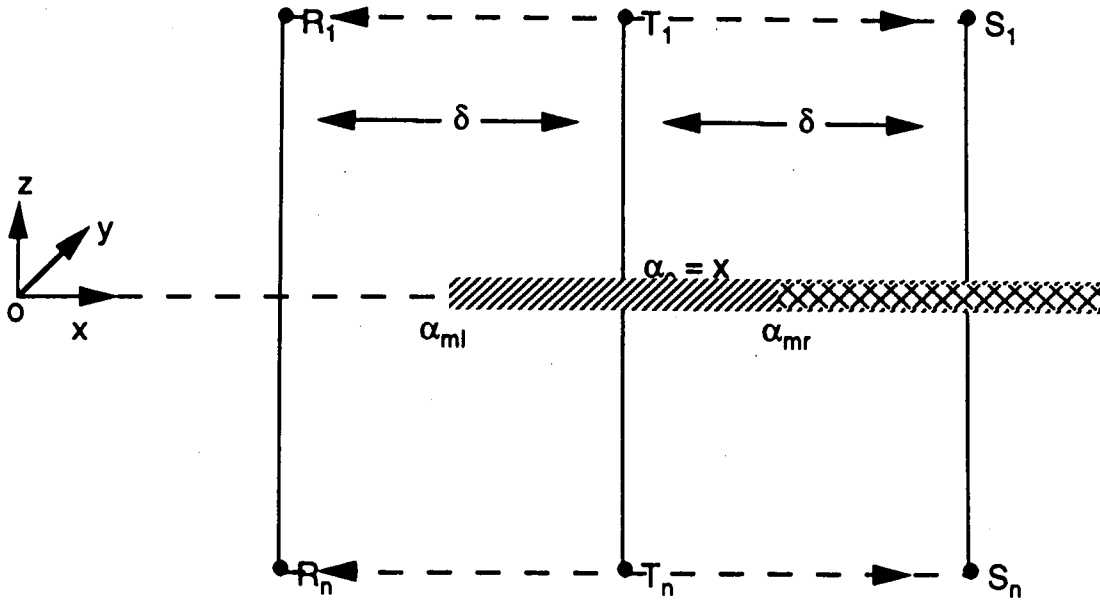


Figure 6. Feasible base locations to reach a surface

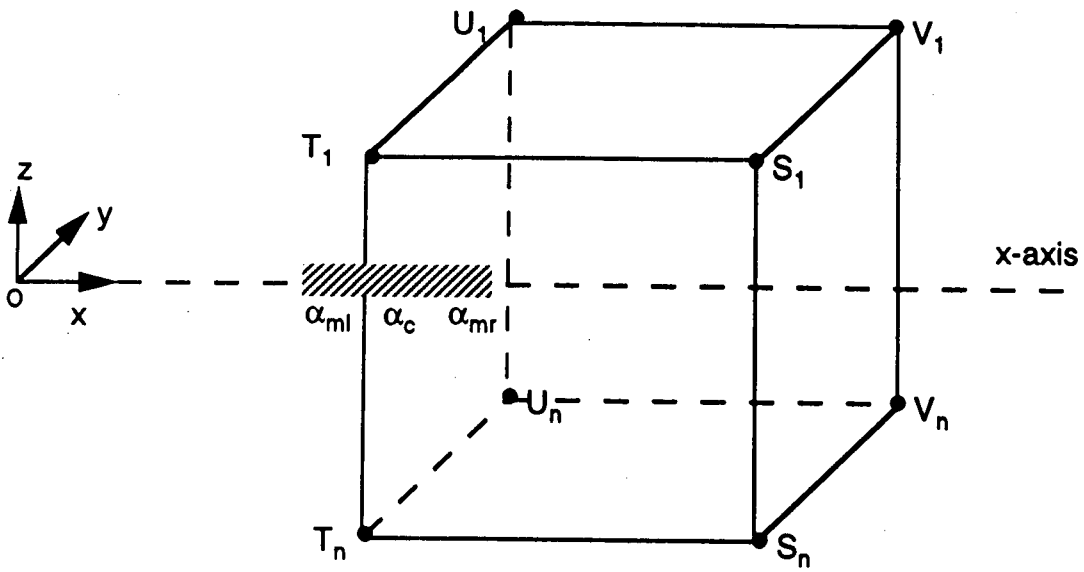


Figure 7. Feasible base locations to reach a volume

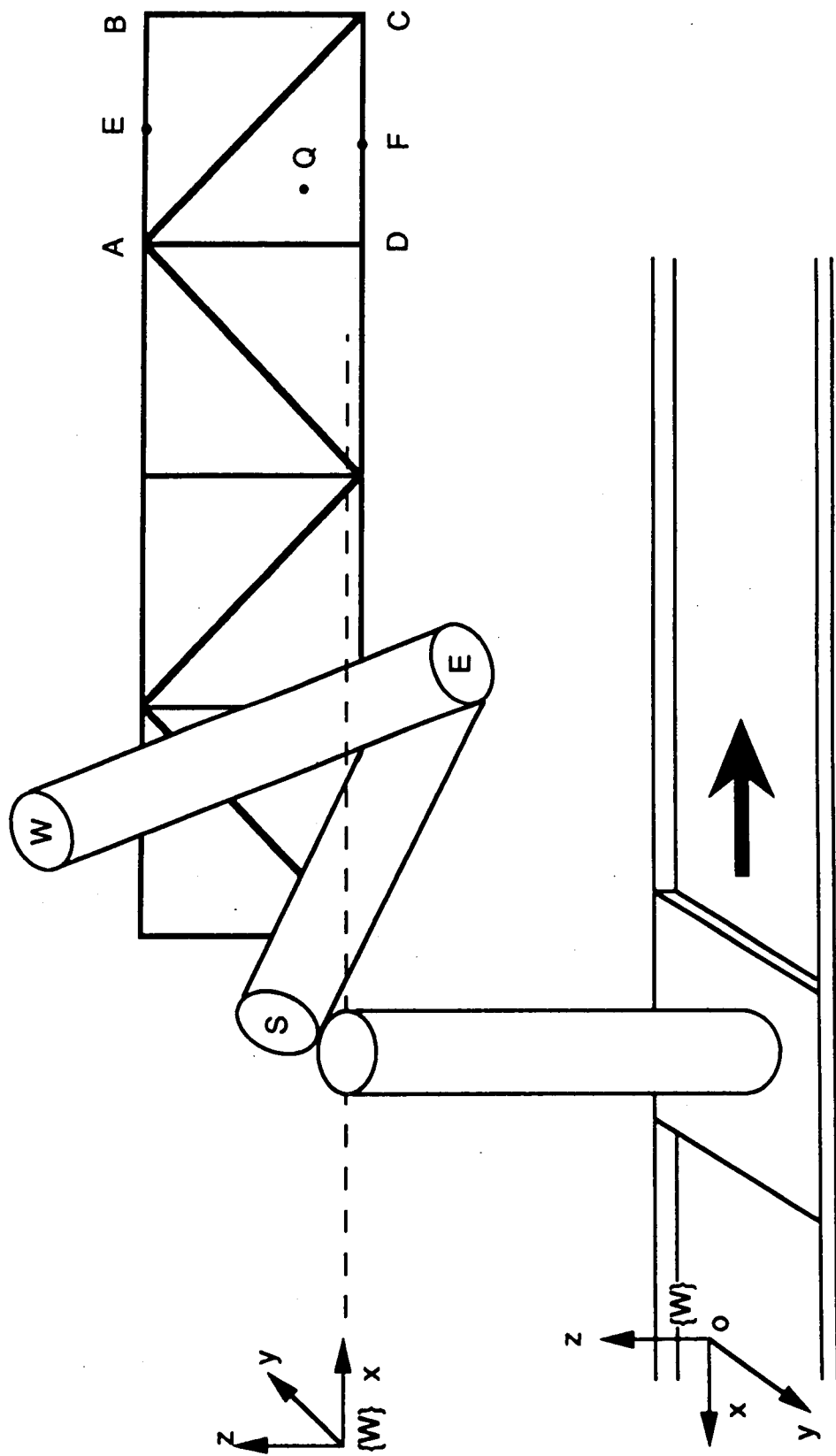


Figure 9. Schematic of the experimental setup

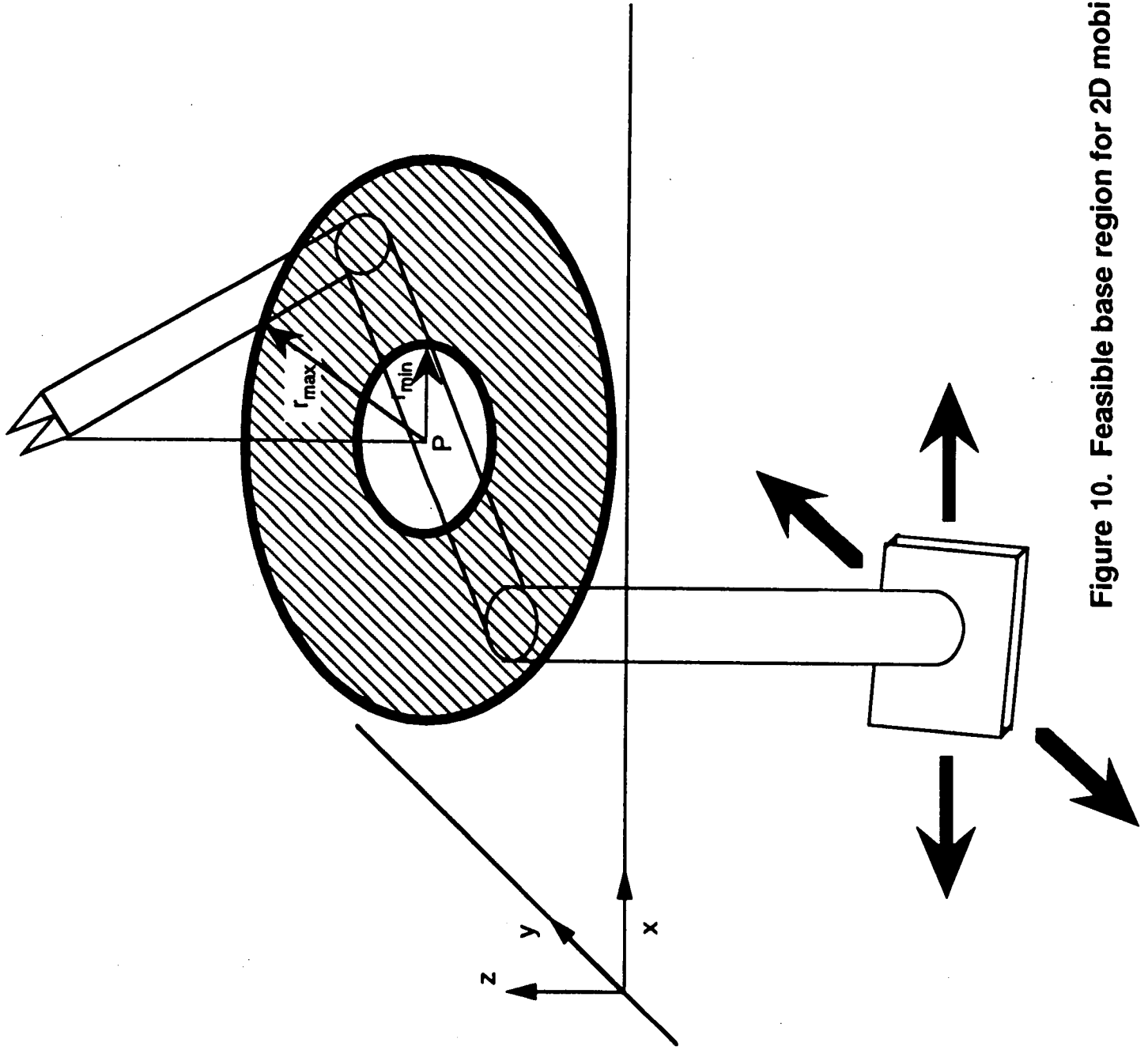


Figure 10. Feasible base region for 2D mobile robots

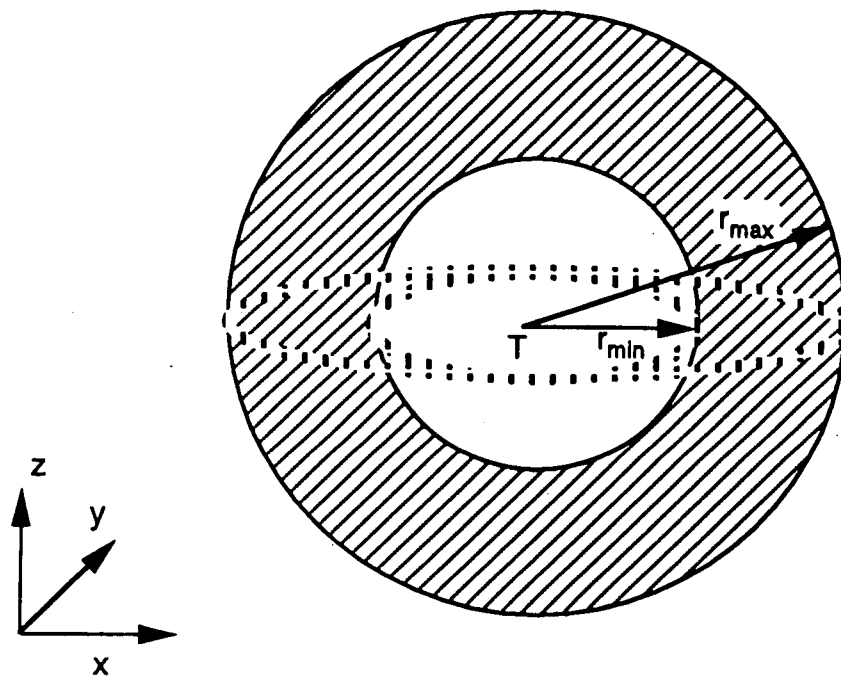


Figure 11. Feasible base region for 3D mobile robots